

**Effect of Geometrical and Physical parameters of
AlGa_N/Ga_N HEMT on the electrical characteristics with AlN spacer layer**

Abdelmalek Douara¹, Abdelaziz Rabehi^{2,3}, Mostefa Hamdani¹

¹Faculty of Science and Technology, Tissemsilt University, Algeria

²Laboratoire de Micro-électronique Appliquée. Université Djillali Liabès de Sidi Bel Abbés,
BP 89, 22000, Sidi Bel Abbés, Algeria

³Ziane Achour University of Djelfa, Djelfa, Algeria

Abstract

The goal of this manuscript is to use the Silvaco Atlas TCAD simulator to investigate the effect of some parameters on the current-voltage characteristics of a high-electron-mobility transistors devices based on Al_xGa_{1-x}N/GaN, Advanced Al_xGa_{1-x}N/AlN/GaN heterostructures with GaN channel layer and AlN spacer layer. It is demonstrated that numerical simulation can be used effectively in the development of HEMTs. We looked into the effect of the GaN thickness layer on the current-voltage characteristics, as well as the effect of the δ -doped layer within Al_xGa_{1-x}N barrier layer, the effect of the spacer thickness is also considered. Among the sample structures we used for our computations, our calculations reveal a low threshold voltage value and the maximum transconductance. Our structure with GaN channel layer thickness of 200 nm, Al content of x = 0.2 with a δ -doped layer of n = 5 x 10¹⁸ cm⁻³, we find that the maximum saturation current.

Keywords: Silvaco Atlas TCAD, Al_xGa_{1-x}N/GaN, δ-doped layer, HEMTs, AlN .

I. Introduction

GaN physical properties make it the most widely used wide bandgap material in active circuit design[1][2]. Its intrinsic qualities (high breakdown fields[3][4], high thermal conductivity, high electron density, good saturation speed[5][6]) give it very good performance at high frequencies [7], whether for power or low noise applications[8] [9].

Historically, the 1990s saw the emergence of a high-bandwidth semiconductor industry with a primary focus

on developing electronic systems for defense applications [10] [11]. The United States and Japan, pioneers in GaN research, are still ahead of Europe In the research of GaN [12], the United States and Japan are still ahead of Europe, whose resources invested in the field are much larger than those deployed in Europe. [13] [14].

The HEMTs based of AlGa_N/Ga_N are of great interest for design of microwave monolithic integrated circuits (satellite receivers, high frequency switches and low power amplifiers ,....) [15] [16] because its properties

are consistent for high frequency and power [17][18].

The first HEMTs transistors appeared in 1980 (Fujitsu, Thomson)[19], where they appeared as an evolution of MESFET (Metal Semiconductor Field Effect Transistor) type transistors made from semiconductors III-V of GaAs type[19] [20]. In 1985, HEMT is presented as a microwave component unique in the world, the first GaN-based transistor (HEMT) appeared in 1993[21].

The proposed structures of Al-GaN/GaN HEMTs devices were improved. In this work we investigate the impact of thickness of the channel (GaN) and doping concentration within (AlGaN) layer on the current-voltage characteristics using The Atlas TCAD simulator, In addition, we are simulating by varied the different important device parameters (Al molar fraction, and thickness of AlN interlayer). Our structure simulated find the maximum drain source saturation current 43 A/m. With a thickness of the channel is 200 nm and existence 15 nm AlN interlayer.

II. Principe of HEMT

Figure.1 shows the principle in a HEMT is the alignment to form a heterojunction of two semiconductor adjacent (AlGaN and GaN) [22] [23]. the donor (carrier supply) of AlGaN layer supplies electrons to the 2-DEG (two-dimensional electron gas)[24] In a typically doped AlGaN / GaN HEMT device [25], The 2DEG was built on the interface $Al_xGa_{1-x}N/GaN$ even if all the layers are grown without doping [26]. In addition, due to piezoelectric effect in the material system[25] [26], the doping contribution to the concentration of the 2DEG sheet carrier is stated to be less than 30 % [27].

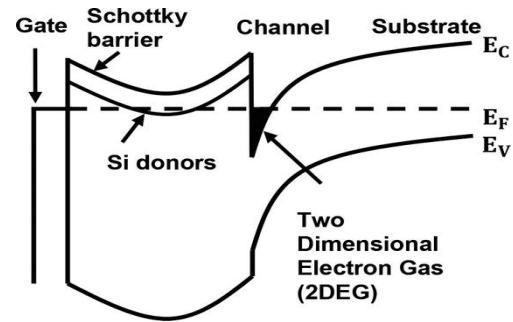


Figure 1. Band diagram of AlGaN/GaN HEMT, at equilibrium [26].

III. Electrical Characteristics

By applying a gate-source voltage to the device. Primarily, the $I-V$ is associated with the sheet carriers density n_s [28]. Indeed, any action on the V_{GS} has the effect of modifying the channel's electronic population which varies the density of the electrons n_s . the current drain-source is given by [29].

$$I_{DS} = W\mu_n q n_s E \quad (1)$$

μ_n : the mobility of carriers.

W : the width of channel layer

As the current is constant in the channel, Eq (1) to be integrated from source - drain. [30] :

$$I_{DS} = \frac{W\mu_n C_0}{L} \left[(V_G - V_{th})V_{DS} - \frac{V_{DS}^2}{2} \right] \quad (2)$$

Where V_{DS} is much lower than $(V_G - V_{th})$, Eq (2) becomes [28] :

$$I_{lin} = W\mu_n C_0 (V_G - V_{th})V_{DS} / L \quad (3)$$

The current of drain -source saturation given by[30]:

$$I_{DS.sat} = \frac{W\mu_n C_0}{2L} (V_G - V_{th})^2 \quad (4)$$

IV. Results and discussions

The $\text{Al}_x\text{Ga}_{1-x}\text{N}/\text{AlN}/\text{GaN}$ HEMT investigated is shown schematically in figure 2, we use 600 nm an insulating substrate (SiC). The channel is made of GaN (UID), the background n-type doping concentration in this layer is $N_{D1} = 10^{15} \text{ cm}^{-3}$, the thickness of the GaN buffer layer was varied in the calculations. The structure consisting of 50 nm an intentionally doped $\text{Al}_x\text{Ga}_{1-x}\text{N}$ barrier layer with a delta-doping profile $N_D(\delta)$ that defines the concentration of electrons in the channel, and this layer on a spacer layer of AlN with various thicknesses with $N_{D2} = 10^{16} \text{ cm}^{-3}$. Also, all structures were simulated with a gate length of $2 \mu\text{m}$ and a source-to-drain spacing of $8 \mu\text{m}$. In addition, for numerical simulation of the electrical output and transfer characteristics, we use the Atlas TCAD simulator software.

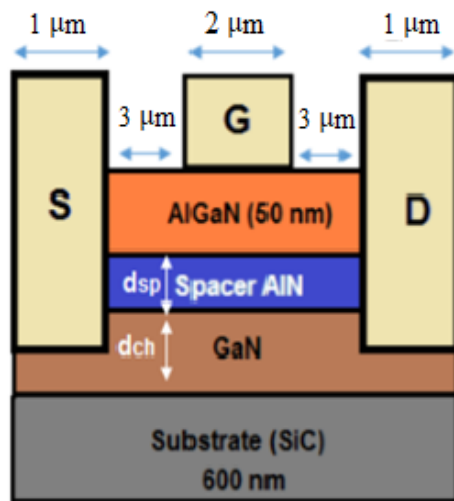


Figure 2. Schematic of $\text{Al}_x\text{Ga}_{1-x}\text{N}/\text{AlN}/\text{GaN}$ HEMT studied.

IV.1. Variation in Thickness of AlN layer

Figure.3 shows calculations of the electrical output characteristics of $\text{Al}_x\text{Ga}_{1-x}\text{N}/\text{GaN}$ HEMT at $V_{GS} = 0$, and we varied a thickness of AlN interlayer with a concentration doping of barrier layer $\text{Al}_{0.2}\text{Ga}_{0.8}\text{N}$ is $N_D(\delta) = 5 \times 10^{18} \text{ cm}^{-3}$. It can be seen that the drain-to-source current is much larger with the existence of AlN layer. This is primarily due to the increased concentration of 2DEG. According to the calculated curves we can observe that the drain-to-source current increases with increasing of the thickness AlN layer. The transfer characteristics of the transistor at $V_{DS} = 0 \text{ V}$ are shown in Figure 4, according to the estimated curves. It has been accomplished here that high electron sheet concentration by reducing impurity scattering, increasing electron mobility within the channel, and increasing device transconductance.

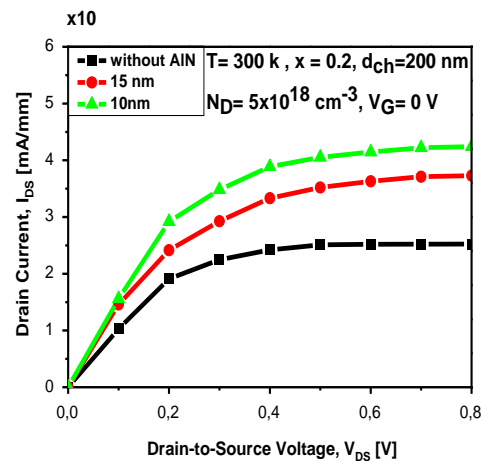


Figure 3. Output characteristics of $\text{Al}_{0.2}\text{Ga}_{0.8}\text{N}/\text{GaN}$ calculated using the Atlas TCAD simulator, for different thickness of AlN at $V_{GS} = 0$.

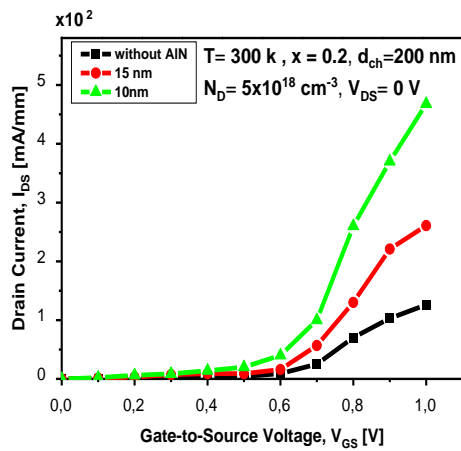


Figure 4. Transfer characteristics of $\text{Al}_{0.2}\text{Ga}_{0.8}\text{N}/\text{GaN}$ calculated using the Atlas TCAD simulator, for different thickness of AlN at $V_{DS} = 0 \text{ V}$.

IV.2. Variation in Thickness of Al-GaN layer

In this section, we have fixed the thickness of AlN at 15 nm, and we varied the thickness of the GaN in the simulation. at $V_G = 0 \text{ V}$. The drain current increases significantly with 200 nm of AlGa_N barrier layer thickness, as can be seen. Simultaneously, a reduction in barrier-layer thickness results in a considerable rise in transconductance. However, despite of the current-collapse effect, a decrease in the drain current in the region of small thicknesses of the AlGa_N barrier layer makes it impossible to achieve a suitably high power density in a transistor made from such a structure. Moreover, the Transfer characteristics at $V_{DS} = 0 \text{ V}$, reported in Figure. 6, according to the curves that have been calculated, the influence of GaN thickness channel is Almost the same parameter AlN spacer layer .

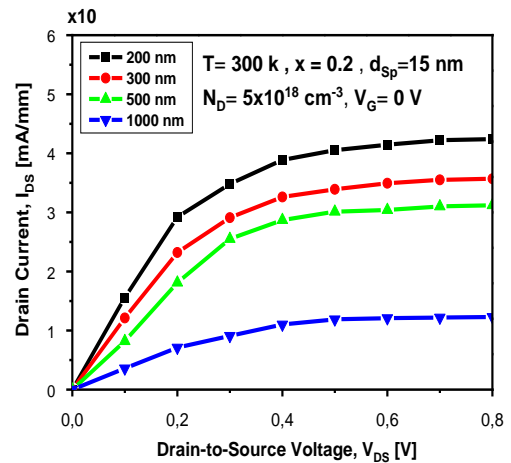


Figure 5. Output characteristics of $\text{Al}_{0.2}\text{Ga}_{0.8}\text{N}/\text{GaN}$ calculated using the Atlas TCAD simulator, for different thickness GaN channel $V_{GS} = 0 \text{ V}$.

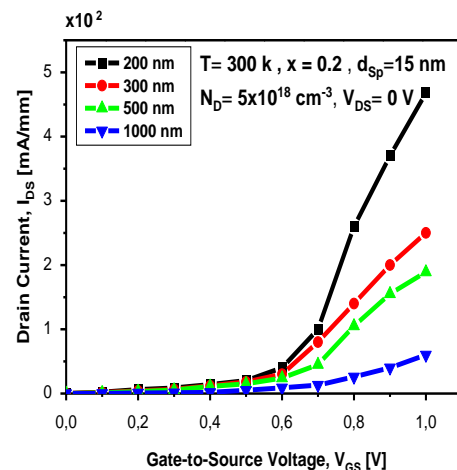


Figure 6. Transfer characteristics of $\text{Al}_{0.2}\text{Ga}_{0.8}\text{N}/\text{GaN}$ using the Atlas TCAD simulator, for different the thickness GaN channel at $V_{DS} = 0 \text{ V}$.

IV.3. Variation Al composition with-in $\text{Al}_x\text{Ga}_{1-x}\text{N}$ the barrier Layer

As shown in figure.7 the results of I_{DS} (V_{DS}) characteristics at $V_{GS} = 0$, We varied the percentages of the aluminum mole (20%, 30%, and 38%), for $x = 0.2$ we find the maximum drain source saturation current of compared with those obtained with $x = 0.3$, and 0.38. Furthermore, the results obtained show that an increase transconductance and

efficiency of HEMT device, and all this we can achieve by varied Al molar fraction in the AlGa_N layer.

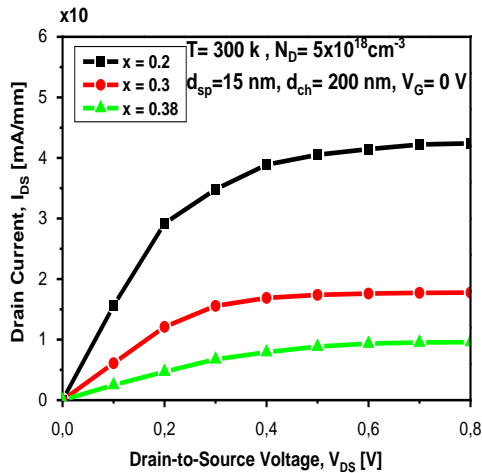


Figure 7. Output characteristics of Al_{0.2}Ga_{0.8}N/GaN calculated using the Atlas TCAD simulator, for different Al molar fraction $V_{GS} = 0$ V.

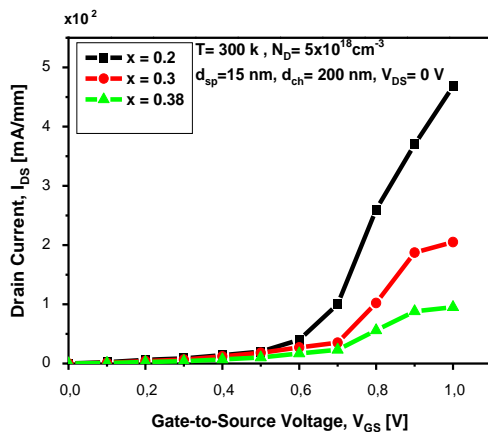


Figure 8. Transfer characteristics of Al_{0.2}Ga_{0.8}N/GaN calculated using the Atlas TCAD simulator, for different Al molar fraction $V_{DS} = 0$ V.

IV.4. Variation in donor concentration within Al_xGa_{1-x}N barrier layer

For the effects of δ -doping on the Al_{0.2}Ga_{0.8}N, the maximum transconductance of HEMTs device depends on the maximum carrier sheet density in the channel at the Al_xGa_{1-x}N/GaN interface, the carriers in the electron

channel are generally transferred from Al_xGa_{1-x}N barrier to the hetero-interface. Therefore, doping of Al_xGa_{1-x}N barrier is necessary to achieve high electron sheet concentration and therewith high device transconductance [18].

We varied the N_D donor concentration within the Al_{0.2}Ga_{0.8}N barrier layer, and fixed other parameters, we obtain our results in figure.9, the results of output characteristics visualize that intentional doping barrier layer is necessary for obtaining high transconductance, the drain-to-source current increases with increasing δ -doping level within the Al_{0.2}Ga_{0.8}N layer, With the highest doping concentration, that is $N_D(\delta) = 5 \times 10^{18} \text{ cm}^{-3}$, the device exhibits the highest drain saturation current as shown in Figure 9.

Additionally, we found that the influence of (N_D) is relatively small as we can see from figure. 10. The results obtained in this work are similar to those obtained by Bouguenna et al [30] who found the same trends in the variation of the current with respect to the donor concentration.

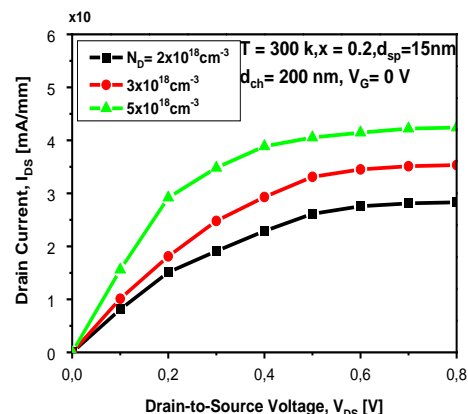


Figure 9. Output characteristics of Al_{0.2}Ga_{0.8}N/GaN calculated using the Atlas TCAD simulator, for different donor concentration in AlGa_N $V_{GS} = 0$ V.

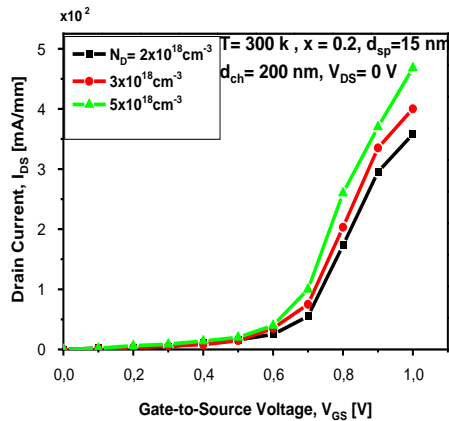


Figure 10. Transfer characteristics of $\text{Al}_{0.2}\text{Ga}_{0.8}\text{N}/\text{GaN}$ calculated using the Atlas TCAD simulator, for different donor concentration $V_{DS} = 0 \text{ V}$.

IV.5. Simulation at different voltages

In this section, figures. 11 and 12 shows current–voltage characteristics with different values of V_{DS} and V_{GS} , respectively. Our calculations were varied from -0.1 V to 0.2 V , with increasing V_G , the increase in the calculated drain voltage. The effect of gate leakage may however be included in the simulations.

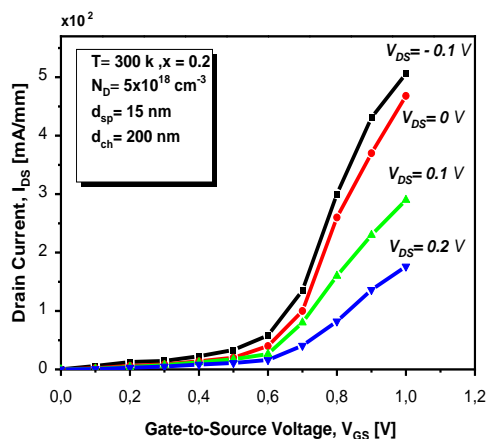


Figure 11. Transfer characteristics of $\text{Al}_{0.2}\text{Ga}_{0.8}\text{N}/\text{GaN}$ calculated using the Atlas TCAD simulator, for different voltage V_{DS} .

The output characteristics results are plotted and a high drain current is observed when the voltage at the gate is lower as shown in figure.11, According to the calculated curves, we find ($I_{D_{\text{Smax}}} = 505 \text{ mA/mm}$ at $V_{DS} = -0.1 \text{ V}$), and the threshold voltage of our structure is 0.5 V when a voltage of drain-to-source is 0 V .

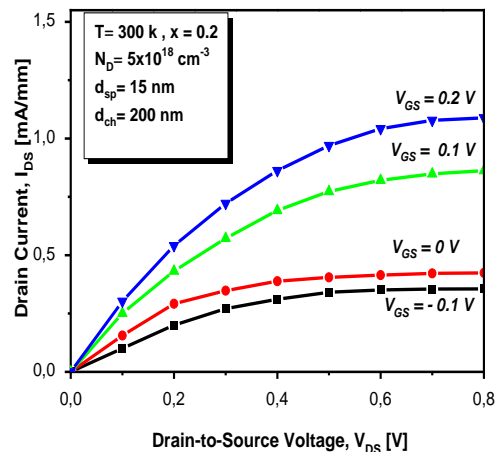


Figure 12. Output characteristics of $\text{Al}_{0.2}\text{Ga}_{0.8}\text{N}/\text{GaN}$ calculated using the Atlas TCAD simulator, for different voltage V_{GS} .

V. Conclusions

In our results of simulation we showed the electrical characteristics of HEMT based of AlGaIn/GaN by the silvaco Atlas simulator. The influence of thickness AlN interlayer on the current-voltage characteristics of AlGaIn/GaN heterostructures has been considered, additional studies related to the influence of other parameters. Our results show a clear field-effect at positive bias voltages with $V_{th} = 0.3 \text{ V}$. The highest of current drain-source dependent with the Al content and the thickness and the donor concentration within AlGaIn barrier layer, for a structure with 15 nm of spacer layer, $N_D(\delta) = 5 \times 10^{18} \text{ cm}^{-3}$, and Al fraction

molar of the barrier layer $x = 20\%$, For this device, the transfer characteristics show a low threshold voltage value and the highest maximum transconductance g_m , the concentration of the donor in the AlGa_N layer is a less significant factor compared to other parameters leading to the change in the current value of in channel.

Conflict of interest

No conflict of interest exists in this manuscript and it has been approved by all authors for publication.

Funding

No funding was received to assist with the preparation of this manuscript.

References

- [1] H. Morkoç, S. Strite, G. B. Gao, M. E. Lin, B. Sverdlov, and M. Burns, "Large-band-gap SiC, III-V nitride, and II-VI ZnSe-based semiconductor device technologies," *J. Appl. Phys.*, vol. 76, no. 3, pp. 1363–1398, 1994.
- [2] P. Perlin, A. Polian, J. P. Itie, I. Grzegory, E. Litwin-Staszewska, T. Suskia, "Physical properties of GaN and AlN under pressures up to 0.5 Mbar" *Physica B: Condensed Matter* Volume 185, 426-427, 1993.
- [3] Y. Dora, A. Chakraborty, L. McCarthy, S. Keller, S. P. Denbaars, and U. K. Mishra, "High breakdown voltage achieved on AlGa_N/Ga_N HEMTs with integrated slant field plates," *IEEE Electron Device Lett.*, vol. 27, no. 9, pp. 713–715, 2006.
- [4] Y. Wang, Y. Ding, and Y. Yin, "Reliability of Wide Band Gap Power Electronic Semiconductor and Packaging: A Review" *Energies* 2022, 15, 6670.
- [5] X. Huang, P. Jiang, and T. Tanaka, "A review of dielectric polymer composites with high thermal conductivity," *IEEE Electr. Insul. Mag.*, vol. 27, no. 4, pp. 8–16, 2011.
- [6] S. Arulkumar, S. Vicknesh, G. I. Ng, Z. H. Liu, S. L. Selvaraj, and T. Egawa, "High vertical breakdown strength in with low specific on-resistance AlGa_N/AlN/Ga_N HEMTs on silicon," *Phys. Status Solidi - Rapid Res. Lett.*, vol. 5, no. 1, pp. 37–39, 2011.
- [7] F. Giannazzo et al., "High-Performance Graphene/AlGa_N/Ga_N Schottky Junctions for Hot Electron Transistors," *ACS Appl. Electron. Mater.*, vol. 1, no. 11, pp. 2342–2354, 2019.
- [8] M. Rudolph, N. Chaturvedi, K. Hirche, J. Würfl, W. Heinrich, and G. Tränkle, "Highly rugged 30 GHz Ga_N low-noise amplifiers," *IEEE Microw. Wirel. Components Lett.*, vol. 19, no. 4, pp. 251–253, 2009.
- [9] A. Ballestín-Fuertes, J. Muñoz-Cruzado-Alba, José F. Sanz-Osorio, and Erika Laporta-Puya "Role of Wide Bandgap Materials in Power Electronics for Smart Grids Applications", *Electronics* 2021, 10, 677.
- [10] D. W. Runton, B. Trabert, J. Shealy, and R. Vetry, "History of Ga_N: High-power RF gallium nitride (Ga_N) from infancy to manufacturable process and beyond," *IEEE Microw. Mag.*, vol. 14, no. 3, pp. 82–93, 2013,

- [11] A. Galetovic, "Patents in the History of the Semiconductor Industry: The Ricardian Hypothesis", Oxford Academic, pages 21-21, P201, 2021
- [12] Tyler J. Flack, Bejoy N. Pushpakaran & Stephen B. Bayne, "GaN Technology for Power Electronic Applications: A Review", Journal of Electronic Materials volume 45, pages 2673–2682 (2016).
- [13] H. Amano, "Growth of GaN Layers on Sapphire by Low-Temperature-Deposited Buffer Layers and Realization of p-type GaN by Magnesium Doping and Electron Beam Irradiation (Nobel Lecture)", *Angew. Chemie - Int. Ed.*, vol. 54, no. 27, pp. 7764–7769, 2015.
- [14] U.K. Mishra, Yi-Feng Wu, B.P. Keller, S. Keller, S.P. Denbaars, "GaN microwave electronics EEE Transactions on microwave theory and techniques," vol. 46, no. 6, June 1998,
- [15] S. Piotrowicz et al., "Overview of AlGaN/GaN HEMT technology for L- to Ku-band applications," *Int. J. Microw. Wirel. Technol.*, vol. 2, no. 1, pp. 105–114, 2010.
- [16] S. Piotrowicz, E. Morvan, R. Aubry, "Overview of AlGaN/GaN HEMT technology for L- to Ku-band applications", *International Journal of Microwave and Wireless Technologies*, 2010, 2(1), 105–114.
- [17] S. Colangeli, A. Bentini, W. Ciccognani, E. Limiti, and A. Nanni, "GaN-based robust low-noise amplifiers," *IEEE Trans. Electron Devices*, vol. 60, no. 10, pp. 3238–3248, 2013.
- [18] C. Sanabria et al., "Influence of epitaxial structure in the noise figure of AlGaIn/GaN HEMTs," *IEEE Trans. Microw. Theory Tech.*, vol. 53, no. 2, pp. 762–768, 2005.
- [19] R. Nandi et al., "A New Field-Effect Transistor with Selectively Doped GaAs / n-Al_xGa_{1-x}As Heterojunctions," vol. 225, no. 17, pp. 1–2, 1980.
- [20] U. M. Constantine, "Analyse des transistors à effet de champ MESFET GaAs," 2009.
- [21] P. Murugapandiyam, V. Rajya Lakshmi, N. Ramkumar, P. Eswaran & Mohd Wasim. "GaN-based high-electron mobility – power and high-frequency application: A review," *Innovations in Electronics and Communication Engineering* 339–348
- [22] S. Colangeli, A. Bentini, W. Ciccognani, E. Limiti, and A. Nanni, "GaN-based robust low-noise amplifiers," *IEEE Trans. Electron Devices*, vol. 60, no. 10, pp. 3238–3248, 2013, doi: 10.1109/TED.2013.2265718.
- [23] Y. Chen, "Nanofabrication by electron beam lithography and its applications: A review," *Microelectron. Eng.*, vol. 135, pp. 57–72, 2015.
- [24] B. J. van Wees, H. van Houten, C. W. J. Beenakker, J. G. Williamson, L. P. "Quantized conductance of point contacts in a two-dimensional electron gas" *Phys. Rev. Lett.* 60, 848 .1988.
- [25] S. Firoz, R. K. Chauhan, and C.

- Engineering, “comparison of algan / gan and algaas / gaas based hemt device under,” *Int. J. Adv. Eng. Technol.*, vol. 1, no. 2, pp. 12–19, 2011.
- [26] M. N. A. Aadit, S. G. Kirtania, and M. K. Alam, “Dependence of threshold voltage on doped layer thickness in AlGa_N/Ga_N HEMT: An improved split donor E-mode design,” 2016 5th Int. Conf. Informatics, Electron. Vision, ICIEV 2016, pp. 681–686, 2016.
- [27] X. G. He, D. G. Zhao, and D. S. Jiang, “Formation of two-dimensional electron gas at AlGa_N/Ga_N heterostructure and the derivation of its sheet density expression,” *Chinese Phys. B*, vol. 24, no. 6, pp. 1–6, 2015.
- [28] A. Douara, B. Djellouli, A. Rabehi, A. Ziane, and N. Belkadi, “I-V Characteristics Model for AlGa_N / Ga_N HEMTs Using Tcad-Silvaco,” *J. New Technol. Mater.*, vol. 4, no. 2, pp. 16–24, 2014.
- [29] A. Douara, A. Rabehi, B. Djellouli, A. Ziane, & H. Abid “2-D optimisation current–voltage characteristics in AlGa_N/Ga_N HEMTs with influence of passivation layer,” *International Journal of Ambient Energy*, Pages 1363-1366.2018
- [30] D. Bouguenna, A. B. Stambouli, A. Zado, D. J. As, and N. M. Maaza, “2D Simulations of Current-voltage Characteristics of Cubic Al_xGa_{1-x}N / Ga_N Modulation Doped Hetero-junction Field Effect Transistor Structures,” vol. 2, no. 5, pp. 309–315, 2012.